

5/7/02



1997 HSR Aerodynamic Performance Workshop

Testing the 2.2% HSR Reference H Model with a Modified Wing Planform in the NTF

Lewis R. Owens, Jr.

NASA LaRC

Richard A. Wahls

NASA LaRC

Marvine P. Hamner

McDonnell Douglas Aerospace

NASA Langley Research Center

February 26, 1997

The HSR program moved into phase two with the selection of a new airplane configuration, the Technology Concept Airplane (TCA). The TCA was designed based on the experiences gained while investigating both the Reference H and the Arrow Wing configurations in different wind tunnels and CFD studies. Part of that investigation included performing extensive high Reynolds number testing on the Reference H configuration in the NTF to provide data for predicting full-scale flight performance, as well as developing techniques for testing these types of configurations in the NTF. With the selection of the TCA configuration, a smaller investigation was designed to examine whether or not the scaling characteristics of the TCA configuration are similar to those observed for the Reference H configuration. This presentation will include a description of the 2.2% Modified Reference H model used in this investigation (highlighting the similarities and the differences when compared to the TCA configuration), the testing objectives, and some preliminary findings that are relevant to the current high-lift system.



Outline

- Objectives
- Background
- Approach
- Model Geometry
- Analysis Approach
- NTF Results
 - planform
 - partial vs full (f/m & minituft)
- Conclusions

As outlined above, this presentation will begin with a statement of the general objectives of the project, followed by background information which led to the initiation of the study, and the approach taken to meet the objectives. Next, the wind tunnel model is described including its relationship to both the Reference H and Technology Concept Airplane (TCA) geometries. Next, the general data analysis approach will be discussed relative to the objectives of this study. Finally, preliminary analysis of results from the experimental part of this study will be discussed. Concluding remarks will close the presentation.



1997 HSR Aerodynamic Performance Workshop

Objectives

- Obtain Rn sensitivity data for representative wing with the TCA planform
- Obtain Rn sensitivity data for partial vs. full inboard LE flap
- Expand subsonic/transonic data base of Rn sensitivities associated with LE radius variations, including the supersonic LE of an outboard wing panel
 - see paper by Wahls, Rivers, & Owens in CA section of this Workshop:
"Prediction and Assessment of Reynolds Number Sensitivities Associated with Wing Leading-Edge Radius Variations"

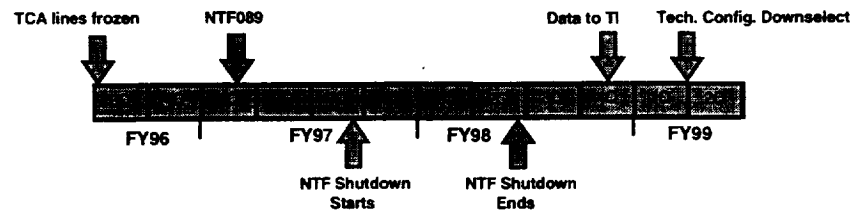
The general objectives of the project are shown above. The primary goals included preliminary assessments of the Rn effects associated with the planform change from the Reference H to the TCA and of the corresponding change to the high-lift, inboard LE flap configuration. An additional objective addressed in the course of this study, but not presented herein, included the expansion of the data base showing the effects of LE radius distribution and corresponding sensitivity to Rn at subsonic and transonic conditions. Particular emphasis was placed on the under exploited supersonic LE of the outboard wing panel. This topic was addressed in the experimental portion of the study, and results are described in a separate paper in this workshop (Configuration Aerodynamics Session) entitled:

"Prediction and Assessment of Reynolds Number Sensitivities Associated with Wing Leading-Edge Radius Variations," by Wahls, Rivers and Owens.



Background

- HSR Program
 - Baseline configuration changed from Ref H to TCA
 - Timing issues
 - affect next downselect to Tech. Configuration
 - material availability, new vs. modified model, NTF shutdown



The HSR program is currently in a 3 year phase centered around the evaluation and redesign of the TCA configuration. It was desired to generate Rn effects data on the TCA planform, examine the high-lift LE flap configuration, and demonstrate that a blunt supersonic LE design is worth pursuing in time to provide input to the definition of the follow-on baseline configuration. Given the NTF schedule and major shutdown for upgrade, model material availability, and insufficient funds/support for a new model, the decision was made to target a test window in the NTF in the 1st quarter of FY97 prior to the NTF shutdown.



Approach

- Modify 2.2% Ref H model to TCA planform
 - include alternate LE radius distribution & high-lift flaps
- Perform NTF test
 - Rn effects assessment on TCA planform
 - compare partial vs full inboard flap differences and associated Rn effects

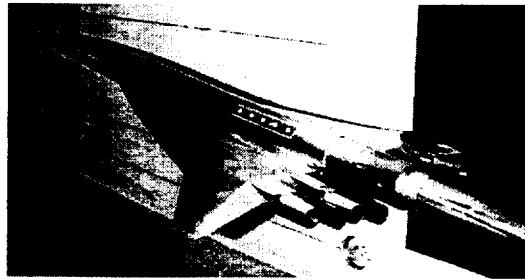


image 1: 1/17/97

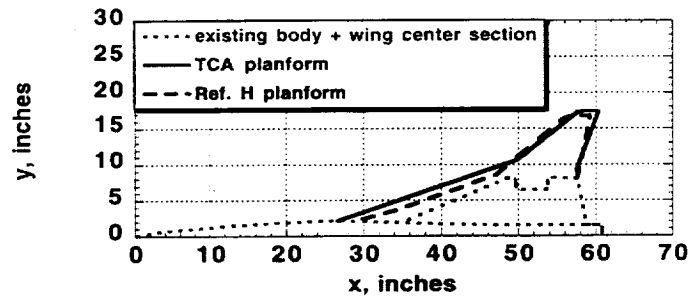
The approach to meet the objectives within the program and facility availability constraints was as follows. First, modify an existing model suitable for the NTF test environment. The obvious choice was the 2.2% HSR Reference H model. Second, perform a test in the NTF at high-lift and transonic conditions to provide a wide range of Rn conditions to allow experimentally based assessments.



Model Geometry I

- Comparison of Modified Ref H and Ref H Models
- Geometric Constants at 2.2% scale

	S_{ref} ft ² (gross)	mac in.	span in.	AR	LE sweep deg
Ref. H	3.674	22.71	34.23	2.21	76/68.5/48
Modified Ref. H.	4.114	25.07	34.65	2.03	71/52

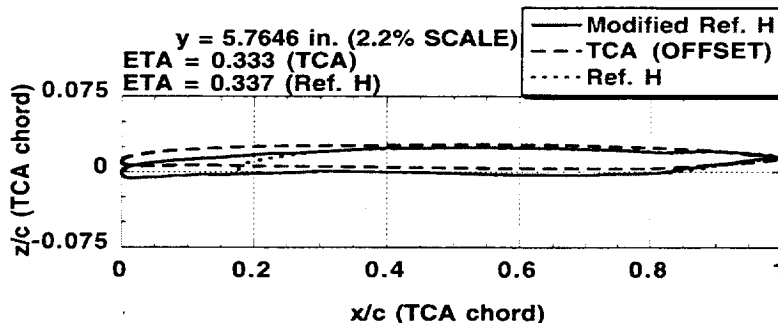


The first step was the modification of the existing 2.2% HSR Ref. H model to represent the TCA wing as closely as possible. Geometric constants are shown above; the Modified Ref. H values are identical to the TCA. Note, that the reference area for the Ref. H is the gross wing area (rather than the wimpres area used during Ref. H testing) to be consistent with the TCA definition. The Ref. H (truncated) body and inboard wing center section and TE (indicated by the dotted lines) were maintained, while the LE and outboard wing panels (indicated by the dashed lines) were not. New LE and outboard wing panels were designed and fabricated to provide the TCA planform while not restricting a return to the Ref. H geometry.



Model Geometry II

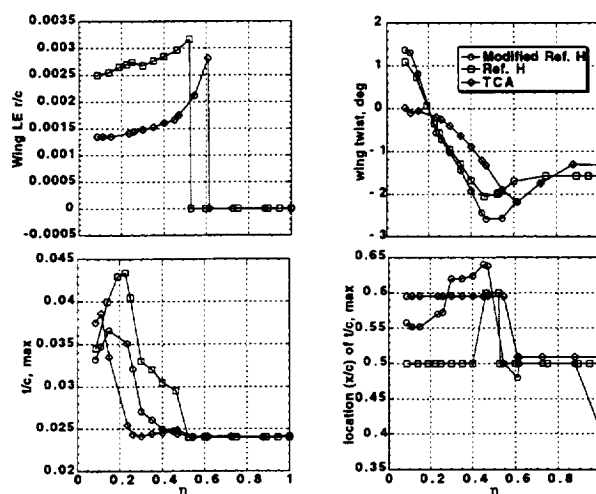
- Airfoil modification process was as follows:
 - align TCA & Ref. H TE (inboard sections; existing model)
 - rotate TCA section around TE to align to with existing Ref. H parts
 - blend overlap section between TCA LE and existing Ref. H parts
 - spanwise blending outboard of existing Ref. H parts



The modification process, or more specifically the blending process, is demonstrated above for a typical inboard airfoil section. First, the TCA section at a given span location is translated to match the TE of the existing Ref. H model hardware. Next, the TCA section is rotated around the TE to align with the existing model parts with emphasis on the upper surface to avoid unwanted surface inflections. Finally, blending occurs over a small region forward of the existing hardware in to the TCA LE region. This sequence was repeated for several airfoils over the span of the existing wing center section/TE hardware; outboard of this point, a small blending region existed in the spanwise direction until the TCA outboard airfoil definitions could be maintained.

Model Geometry III

- Comparison of Modified Ref. H, Ref. H, & TCA Geometries



The resulting geometry had the characteristics shown above. Note that wing LE radius distribution of the modified Ref. H is identical to that of the TCA, and that both the TCA and the Ref. H have a sharp LE on the outboard wing panel. Existing Ref. H model hardware inboard drives the differences in wing twist, maximum thickness, and the location of the maximum thickness. Outboard of the pre-existing hardware, the modified Ref. H and TCA geometries more closely match.

The resulting geometry was smooth and sufficient to address the objectives of the study. However, in no way should this geometry be considered optimized aerodynamically.



1997 HSR Aerodynamic Performance Workshop

NTF Test Variables

- | | |
|--|--|
| • Mach = 0.30 | • Mach = 0.90 |
| • $Rn_{mac} = 9.4 \rightarrow 100 \times 10^6$ | • $Rn_{mac} = 11 \rightarrow 89 \times 10^6$ |
| • $\alpha = -3^\circ \rightarrow 24^\circ$ | • $\alpha = -2^\circ \rightarrow 12^\circ$ |
| • nacelles on/off | • nacelles off |
| • 0/0 flaps | • 0/0 flaps |
| • 30/10 partial & full span flaps | |
| • baseline & alt. LE radius | • baseline & alt. LE radius |

The range of test conditions in the NTF test (designated NTF089) pertinent to this study are shown above. All data shown herein were obtained with natural transition on the wing. A complete set of low Rn data with fixed transition was planned but not obtained due to significant facility downtime associated with a pitch system failure. Force and moment data were obtained. Limited pressure data on the existing Ref. H wing center section were also obtained; LE and outboard wing panel pressures were not obtained due to limited funding and design/fabrication time constraints.



Analysis Approach

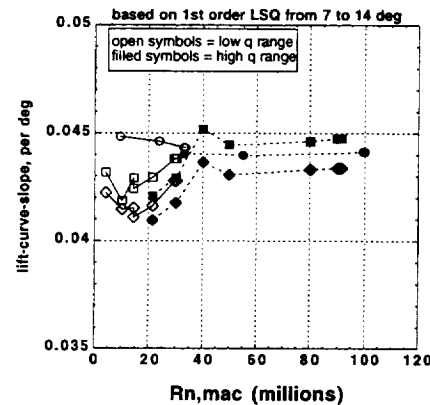
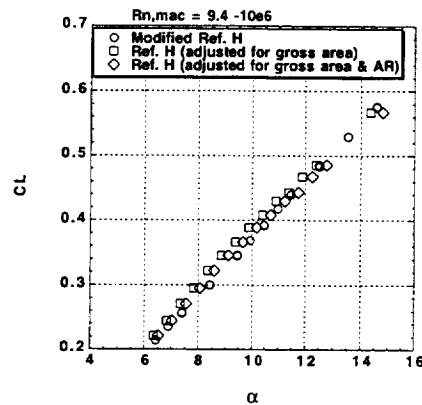
- Differences in Ref. H & Modified Ref. H (TCA planform)
 - AR, camber + twist = warp, wetted area, thickness distrib.,
- Linear Theory
 - simple planform (AR) relationship allows lift-curve-slope comparisons
 - $$\alpha_{M Re H} = \alpha_{Re H} + \frac{C_L}{\pi} \times \left(\frac{1}{AR_{M Re H}} - \frac{1}{AR_{Re H}} \right) \times \frac{180}{\pi}$$
- Plan to use AERO2S for warp effects
 - drag, pitching-moment, $\alpha_{zero-lift}$,
- Compare partial vs full inboard LE flap configuration
 - force & moment data as a function of R_n
 - minituft flow visualization

The analysis approach (work in progress) is outlined above. In order to make comparisons between the R_n trends associated with the Ref. H and those of the modified Ref. H configurations, it is necessary to account for differences in the data due to certain geometric differences. This is a challenging task, and currently only the CL data for the undeflected flaps have been adjusted for AR differences so that comparisons in the lift-curve slope are presented. The AR adjustments are only made to the angle of attack as shown above. Note that this method assumes fully-attached flow, which is not true across the angle-of-attack range tested here. The future analysis plans include modelling camber, twist and wetted-area differences to allow comparisons for drag and L/D. The analysis of the data obtained for the different high-lift flap configurations included making comparisons using the force/moment data as well as the minituft data.



NTF Results I

- Comparison of lift-curve-slope between Ref H & Modified Ref H
 - Mach = 0.3, undeflected flaps
- CL_α trends with Rn differ

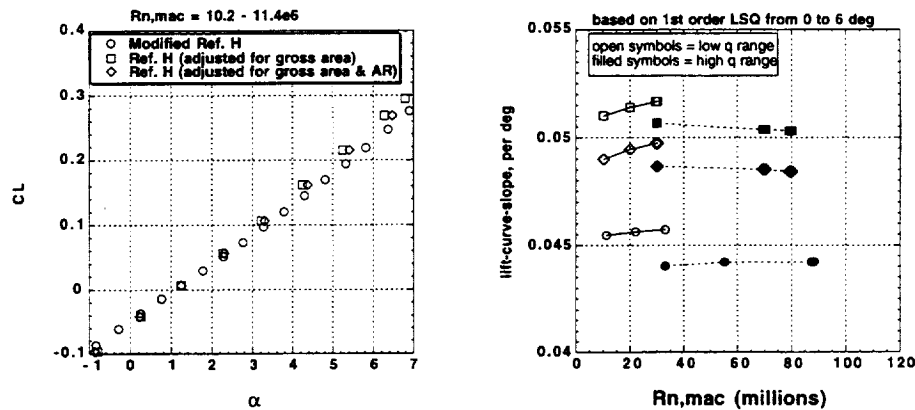


The plot on the left shows the comparison of CL as a function of α for the modified Ref. H, Ref. H (adjusted for gross wing ref. area difference), and Ref. H (adjusted for gross wing ref. area and aspect ratio difference) at low Rn . All data shown is for Mach = 0.3 with undeflected flaps. The aspect ratio correction does not fully collapse the differences between the modified Ref. H and the Ref. H lift curves, which may be expected with various LE separations present in this angle-of-attack range. The plot on the right indicates that the lift-curve slopes obtained from a limited angle-of-attack range for modified Ref. H and Ref. H have different sensitivities to Rn , with the Ref. H data showing more sensitivity at low Reynolds numbers.



NTF Results II

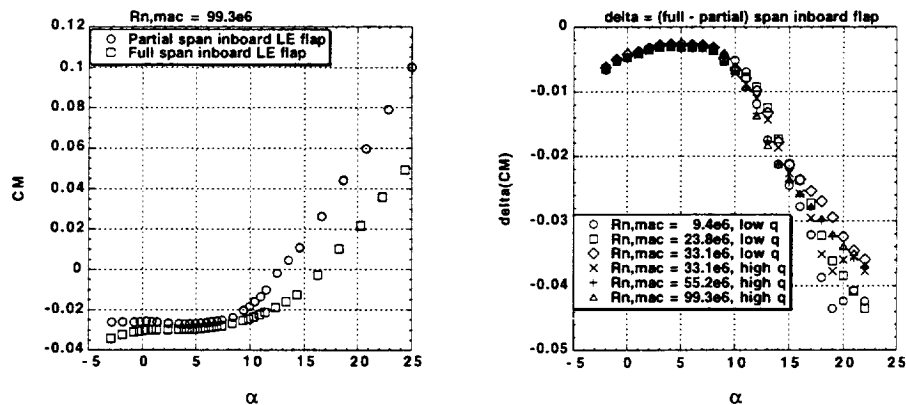
- Comparison of lift-curve-slope between Ref H & Modified Ref H
 - Mach = 0.9, undeflected flaps
- CL_α trends with Rn are similar



The plot on the left shows the comparison of CL as a function of alpha for the modified Ref. H, Ref. H (adjusted for gross wing ref. area difference), and Ref. H (adjusted for gross wing ref. area and aspect ratio difference) at low Rn . All data shown is for Mach = 0.9 with undeflected flaps. The aspect ratio correction does not fully collapse the differences between the modified Ref. H and the Ref. H lift curves, which may be expected with various LE separations present for alpha greater than approximately 2.5 degrees. The plot on the right indicates that the lift-curve slopes obtained from a limited angle-of-attack range for modified Ref. H and Ref. H have similar sensitivities (small) to Rn . The jump in the lift-curve slope at Rn of about 30 million is associated with the aeroelastic step.

NTF Results III

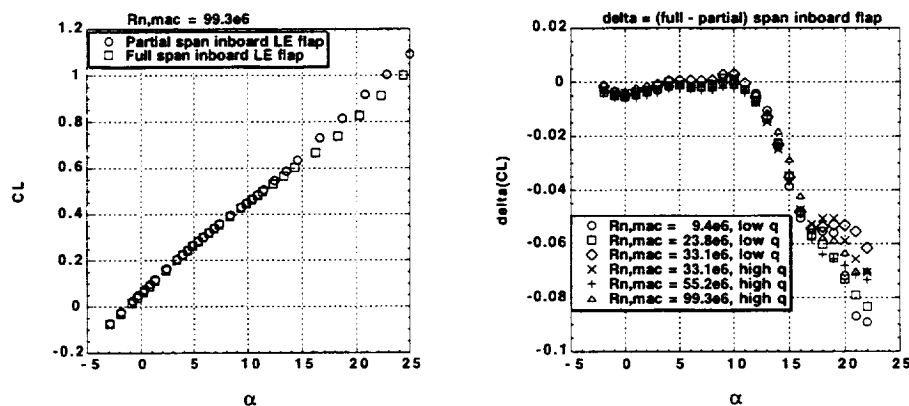
- Comparison of partial vs full inboard flap deployment on CM
 - Large flap configuration effect
 - Small Reynolds number effect (at least relatively)



The plot of CM as a function alpha is presented on the left to show the LE flap configuration (partial span vs full span) effect at the highest available Rn test condition. On the right, a plot of the CM difference (full - partial) as a function of alpha demonstrates that the Rn sensitivities are much smaller than the flap configuration effect.

NTF Results IV

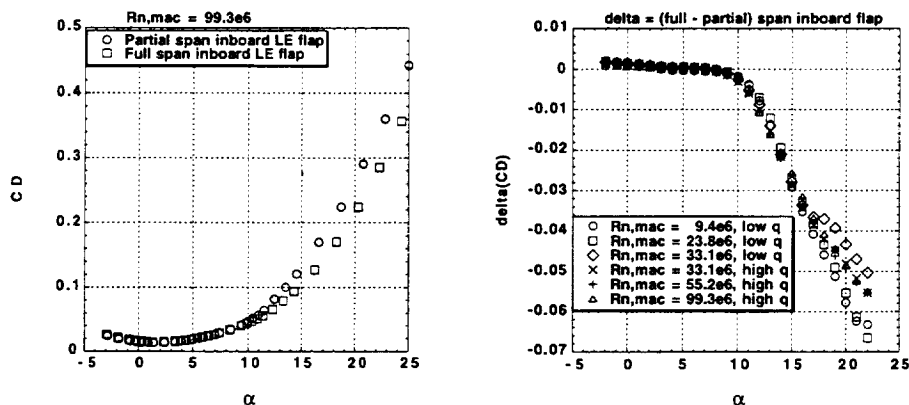
- Comparison of partial vs full inboard flap deployment on CL
 - Large flap configuration effect
 - Small Reynolds number effect (at least relatively)



The plot of CL as a function alpha is presented on the left to show the LE flap configuration (partial span vs full span) effect at the highest available Rn test condition. On the right, a plot of the CL difference (full - partial) as a function of alpha demonstrates that the Rn sensitivities are much smaller than the flap configuration effect.

NTF Results V

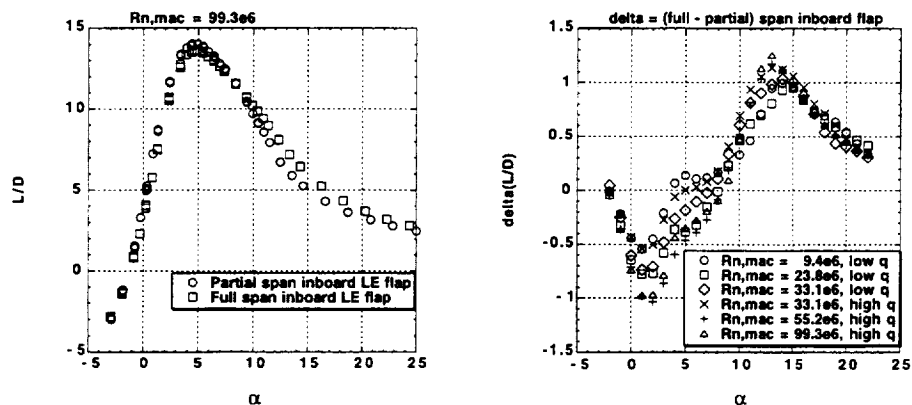
- Comparison of partial vs full inboard flap deployment on CD
 - Large flap configuration effect
 - Small Reynolds number effect (at least relatively)



The plot of C_D as a function α is presented on the left to show the LE flap configuration (partial span vs full span) effect at the highest available Rn test condition. On the right, a plot of the C_D difference (full - partial) as a function of α demonstrates that the Rn sensitivities are much smaller than the flap configuration effect.

NTF Results VI

- Comparison of partial vs full inboard flap deployment on L/D
 - Large flap configuration effect
 - Small Reynolds number effect (at least relatively)

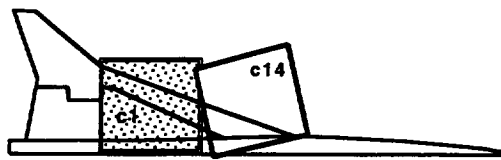


The plot of L/D as a function alpha is presented on the left to show the LE flap configuration (partial span vs full span) effect at the highest available Rn test condition. On the right, a plot of the L/D difference (full - partial) as a function of alpha demonstrates that the Rn sensitivities are smaller than the flap configuration effect.

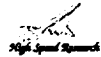


Camera Views of Minitufts on Wing

- Minitufts applied to left upper wing surface only
 - Camera #14
 - inboard LE near wing/body juncture
 - Camera #1
 - mid span LE covering area where part span LE flap begins
 - Camera #9
 - overall view of wing including outboard wing panel
 - not shown in this presentation

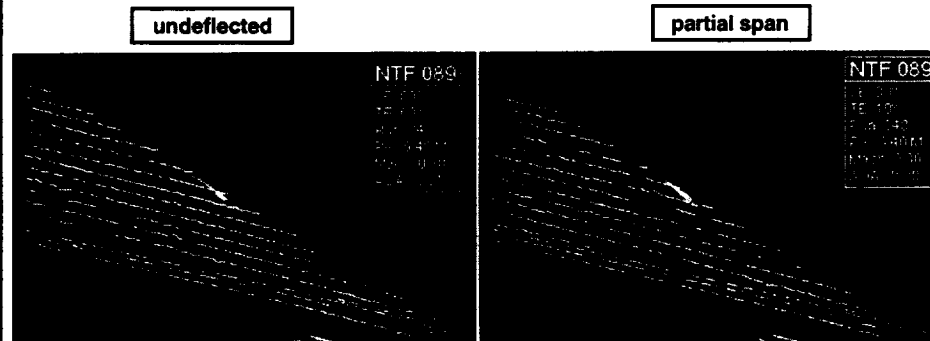


The figure above shows the view orientations for each of the cameras used to obtain minituft data on the inboard, upper surface of the left wing for the modified Ref. H model. The data was obtained at low R_n conditions only. Also, only the $Mach = 0.3$ data is presented in the next slides to illustrate differences associated with the large LE flap effects shown previously in the force/moment data. The data are grouped by nominal angles of attack (8, 12 and 14 degrees). Multiple angles of attack are presented to give a sense of LE vortex progression.



NTF Results VII-a

- Undelected flap vs. partial span flap ($\alpha=8^\circ$)
 - c14; inboard near wing/body juncture
 - both LEs -- attached flow character

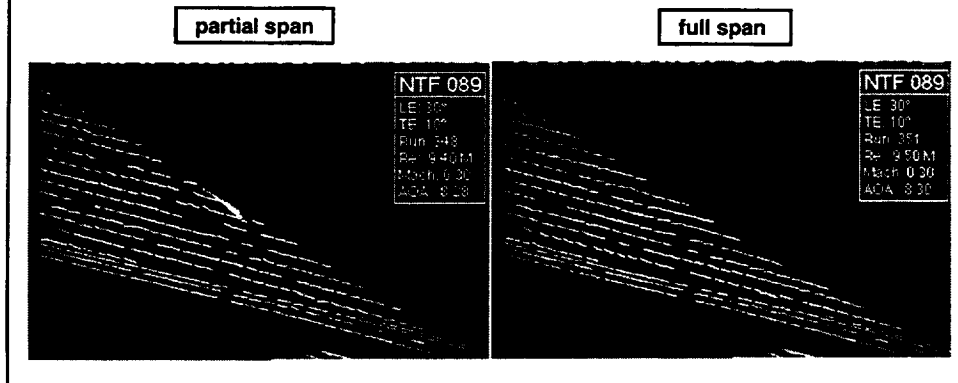


In this figure, the undelected and partial span LE flaps are compared at an alpha of about 8 degrees. Both configurations exhibit attached LE flow characteristics in this region.



NTF Results VII-b

- Partial span flap vs. full span flap ($\alpha=8^\circ$)
 - c14; inboard near wing/body juncture
 - both LEs -- attached flow character



In this figure, the partial and full span LE flaps are compared at an alpha of about 8 degrees. Again, both configurations exhibit attached LE flow characteristics in this region.

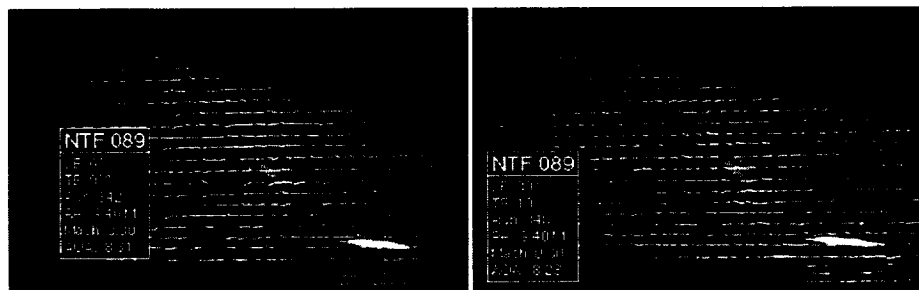


NTF Results VII-c

- Undelected flap vs. partial span flap ($\alpha=8^\circ$)
 - c01; mid span (inboard of LE crank)
 - undelected
 - separated flow character beginning
 - partial span
 - attached flow character on LE flap

undelected

partial span



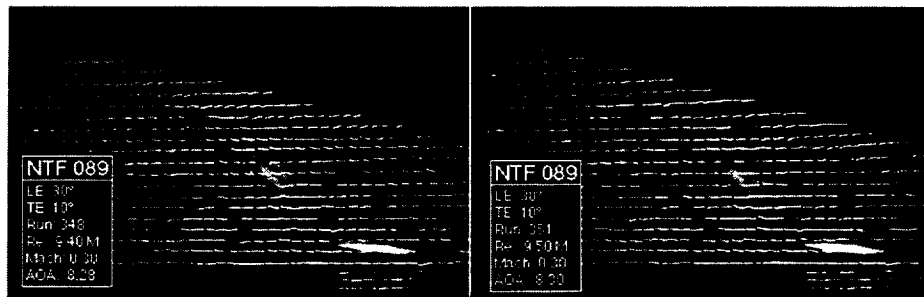
In this figure, the undelected and partial span LE flaps are compared at an alpha of about 8 degrees. The undelected configuration image shows signs of a LE vortex (toward upper, left corner of image). The minitufts that are influenced by separated flow can be identified as those that are not only misaligned with the streamwise direction but must also appear to be a faint blur in the image indicating the dynamic motions of the separated flow. The part span flap does not show any signs of separation.

NTF Results VII-d

- Partial span flap vs. full span flap ($\alpha=8^\circ$)
 - c01; mid span (inboard of LE crank)
 - part span LE
 - attached flow character on LE flap
 - full span LE
 - attached flow character on LE flap

partial span

full span



In this figure, the partial and full span LE flaps are compared at an alpha of about 8 degrees. Both configurations exhibit attached LE flow characteristics in this region.

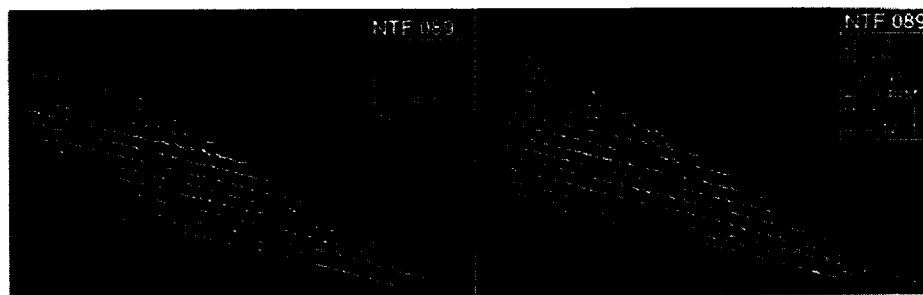


NTF Results VIII-a

- Undelected flap vs. partial span flap ($\alpha=12^\circ$)
 - c14; inboard near wing/body juncture
 - both LEs -- separated flow character beginning

undelected

partial span

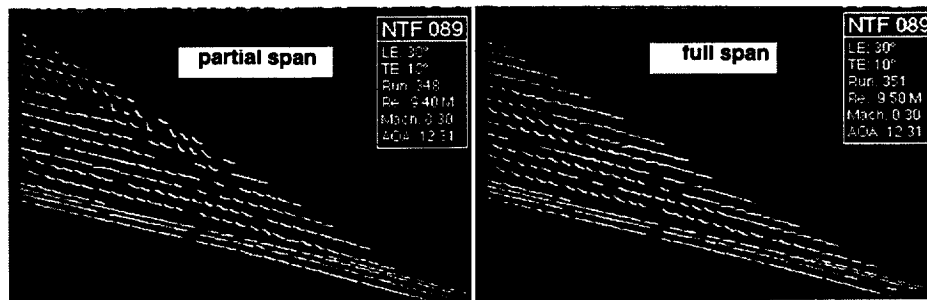


In this figure, both LE configurations exhibit similar LE separation characteristics at this angle of attack.



NTF Results VIII-b

- Partial span flap vs. full span flap ($\alpha=12^\circ$)
 - c14; inboard near wing/body juncture
 - part span LE
 - separated flow character on undeflected inboard LE beginning
 - full span LE
 - attached flow character on LE flap
 - separated flow character at flap hingeline

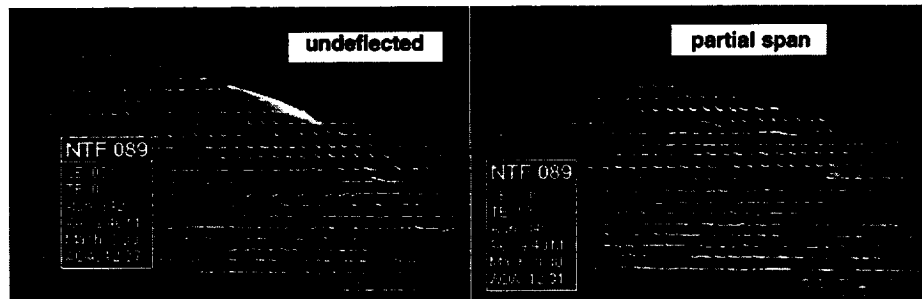


In this figure, the partial and full span LE flap configurations are compared and there is a significant difference in the LE separation characteristics. The flow is attached on the full span LE flap. This difference helps to explain the performance difference between the two flaps, in which the full span flap has lower drag, lower lift, higher L/D and less pitch-up.



NTF Results VIII-c

- Undelected flap vs. partial span flap ($\alpha=12^\circ$)
 - c01; mid span (inboard of LE crank)
 - undelected
 - separated flow character established
 - partial span
 - separated flow character on LE flap
 - separated flow inboard of start of part span flap

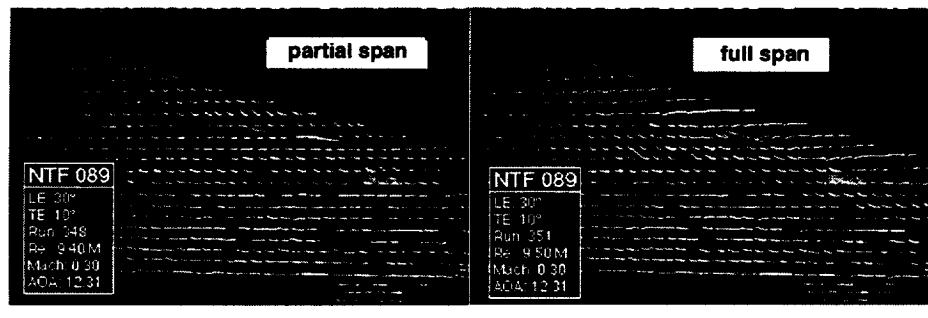


In this figure, the undelected and partial span LE flap configurations are compared and there is a significant difference in the LE separation characteristics. Note that the comparison of these LE configurations looked very similar in the view near the wing/body juncture. (NTF Results VIII-a slide)



NTF Results VIII-d

- Partial span flap vs. full span flap ($\alpha=12^\circ$)
 - c01; mid span (inboard of LE crank)
 - part span LE
 - entire LE flap flow separated
 - full span LE
 - separated flow character on beginning on LE flap
 - separated flow character at flap hingeline



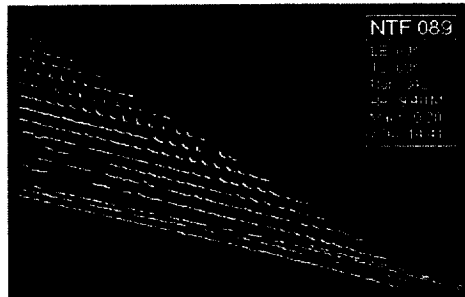
In this figure, the partial and full span LE flap configurations are compared and there is a significant difference in the LE separation characteristics. Again, the full span LE flap has a larger region of attached flow, which helps to explain the performance difference seen in the force/moment data.



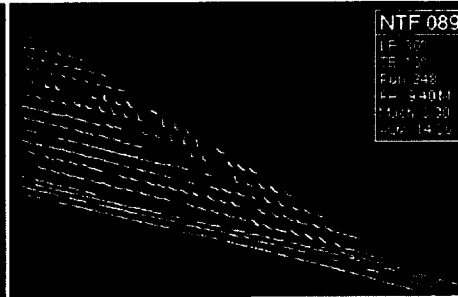
NTF Results IX-a

- Undelected flap vs. partial span flap ($\alpha=14^\circ$)
 - c14; inboard near wing/body juncture
 - both LEs -- separated flow character established

undelected



partial span

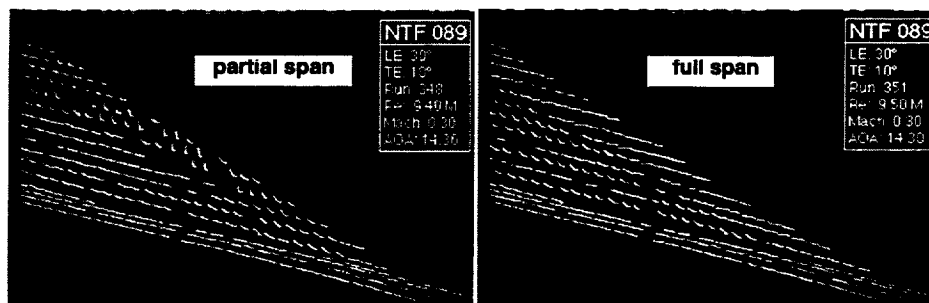


At an angle of attack of 14 degrees, this LE flap comparison is similar to that discussed for 12 degrees. These images were included to give a sense of the LE vortex progression.



NTF Results IX-b

- Partial span flap vs. full span flap ($\alpha=14^\circ$)
 - c14; inboard near wing/body juncture
 - part span LE
 - separated flow character on undeflected inboard LE established
 - full span LE
 - attached flow character on LE flap
 - separated flow character at flap hingeline

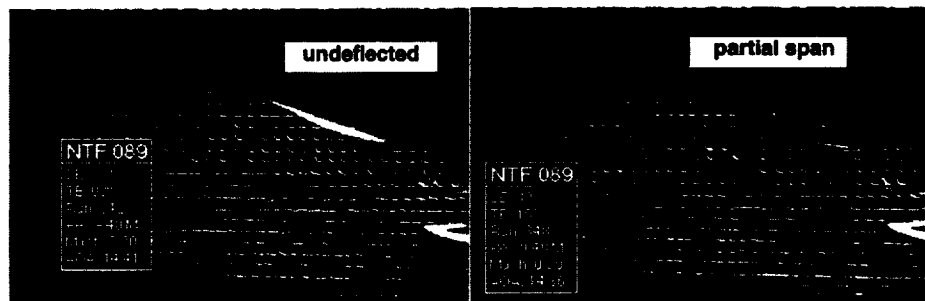


At an angle of attack of 14 degrees, this LE flap comparison is similar to that discussed for 12 degrees. These images were included to give a sense of the LE vortex progression.



NTF Results IX-c

- Undelected flap vs. partial span flap ($\alpha=14^\circ$)
 - c01; mid span (inboard of LE crank)
 - undelected
 - separated flow character established
 - partial span
 - separated flow character on LE flap
 - separated flow inboard of part span flap affects larger area

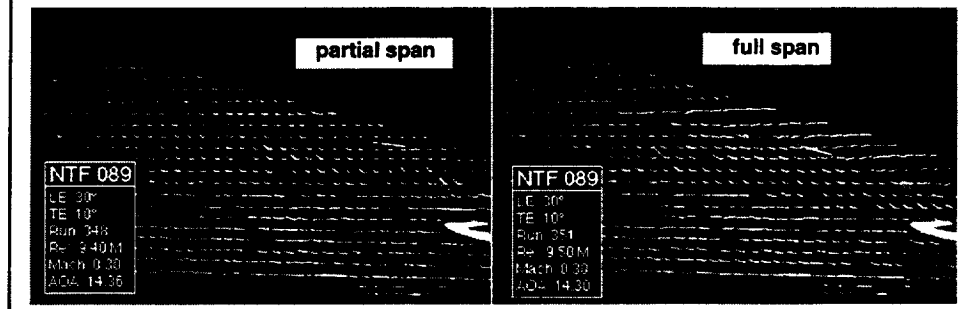


At an angle of attack of 14 degrees, this LE flap comparison is similar to that discussed for 12 degrees. These images were included to give a sense of the LE vortex progression.



NTF Results IX-d

- Partial span flap vs. full span flap ($\alpha=14^\circ$)
 - c01; mid span (inboard of LE crank)
 - part span LE
 - separated flow region of LE continues to grow
 - full span LE
 - separation onset moves inboard on LE flap
 - separated flow character at flap hingeline



At an angle of attack of 14 degrees, this LE flap comparison is similar to that discussed for 12 degrees. These images were included to give a sense of the LE vortex progression.



Conclusions

- Planform Effects (Modified Ref. H vs Ref. H) - 0/0 flaps
 - effectiveness of AR adjustment
 - in general, does not collapse lift curve data
 - CL_{α} trends with Rn
 - Differ at Mach = 0.3
 - Similar at Mach = 0.9
- Partial vs Full Inboard Flap Differences
 - Large performance difference beginning near design condition
 - Rn effect relatively small in comparison to performance difference
 - Differences driven by separation and vortex formation that Rn changes do not eliminate

In conclusion, the analysis of the planform effects has started with an attempt to adjust the lift data for aspect ratio differences for the undeflected flap configurations. These aspect ratio adjustments have not successfully collapsed the lift-curve data. The lift-curve slope trend with Rn depended on the configuration and Mach number. Further analysis of these planform effects are needed as well as looking at deflected flap configurations.

A large performance difference between partial and full span LE flap configurations was found near the design conditions. The data obtained for each flap configuration showed a relatively small (when compared to the performance difference) Rn effect. The LE flap configuration performance difference is explained by the differences in the amount of attached LE flow regions present on each flap.